



WAKE FOREST
UNIVERSITY

Office of Research and Sponsored Programs

April 27, 2017

Office of Naval Research
875 N. Randolph Street
Arlington, VA 22203-1995

Re: Grant # N00014-15-1-2943

To Whom It May Concern:

Enclosed, please find the Final Technical Report and SF298 form for the grant referenced above.

Should you have any questions or need additional information, please feel free to contact me.

Sincerely,

A handwritten signature in black ink that reads "Lori Gabriel".

Lori Gabriel
Director

Cc: James Armistead
Defense Technical Information Center ✓
ONR Patent Office
Naval Research Laboratory
ONR REG Office Atlanta

REPORT DOCUMENTATION PAGE

Form Approved
OMB No. 0704-0188

The public reporting burden for this collection of information is estimated to average 1 hour per response, including the time for reviewing instructions, searching existing data sources, gathering and maintaining the data needed, and completing and reviewing the collection of information. Send comments regarding this burden estimate or any other aspect of this collection of information, including suggestions for reducing the burden, to Department of Defense, Washington Headquarters Services, Directorate for Information Operations and Reports (0704-0188), 1215 Jefferson Davis Highway, Suite 1204, Arlington, VA 22202-4302. Respondents should be aware that notwithstanding any other provision of law, no person shall be subject to any penalty for failing to comply with a collection of information if it does not display a currently valid OMB control number.

PLEASE DO NOT RETURN YOUR FORM TO THE ABOVE ADDRESS.

1. REPORT DATE (DD-MM-YYYY) 04/25/2017			2. REPORT TYPE Final technical report		3. DATES COVERED (From - To) 09/01/2015 – 10/31/2016	
4. TITLE AND SUBTITLE Organic/Inorganic Hybrid Perovskite FETs for Electrically-Injected Laser Action					5a. CONTRACT NUMBER	
					5b. GRANT NUMBER ONR N00014-15-1-2943	
					5c. PROGRAM ELEMENT NUMBER	
6. AUTHOR(S) Oana D. Jurchescu (Co-PI Z. Valy Vardeny, U Utah, under a different grant number)					5d. PROJECT NUMBER	
					5e. TASK NUMBER	
					5f. WORK UNIT NUMBER	
7. PERFORMING ORGANIZATION NAME(S) AND ADDRESS(ES) Wake Forest University Department of Physics 1834 Wake Forest Rd Winston-Salem, NC 27109					8. PERFORMING ORGANIZATION REPORT NUMBER	
9. SPONSORING/MONITORING AGENCY NAME(S) AND ADDRESS(ES) Office of Naval Research					10. SPONSOR/MONITOR'S ACRONYM(S) ONR	
					11. SPONSOR/MONITOR'S REPORT NUMBER(S)	
12. DISTRIBUTION/AVAILABILITY STATEMENT Approved for public release: distribution unlimited.						
13. SUPPLEMENTARY NOTES						
14. ABSTRACT This project will advance the development of the hybridorganic/inorganic halide perovskites (HOIHP by answering fundamental scientific questions with ramifications on potential applications of these materials. We will study the charge transport in HOIHP films and single crystals field-effect transistors (FETs); the magnetic-field-effect on current and electro-luminescence in these devices; and laser action aimed towards current injecting laser. For these studies we will use cw, transient and laser action techniques on electrostatically gated devices.						
15. SUBJECT TERMS						
16. SECURITY CLASSIFICATION OF:			17. LIMITATION OF ABSTRACT	18. NUMBER OF PAGES	19a. NAME OF RESPONSIBLE PERSON	
a. REPORT	b. ABSTRACT	c. THIS PAGE			19b. TELEPHONE NUMBER (Include area code)	
U	U	U	UU	12		



Office of Naval Research (ONR)

Final grant report

ONR N00014-15-1-2943

**Organic/Inorganic Hybrid Perovskite FETs for
Electrically-Injected Laser Action**

PI, Oana D. Jurchescu, Wake Forest University

In collaboration with Z. Valy Vardeny (University of Utah)

– supported under N00014-15-1-2524 ONR grant

Accomplishments

What were the major goals and objectives of the project?

Hybrid organic-inorganic solar cells based on the semiconductor methyl-ammonium (MA) lead halide perovskites, MAPbX_3 (where $\text{X}=\text{Cl}, \text{Br}, \text{I}$) has recently and quite rapidly emerged as one of the most promising contenders for larger scale photovoltaic energy generation. These materials, while solution processed at low temperature, exhibit a remarkable set of materials properties necessary for high efficiency thin film optoelectronic applications. This project aimed to advance the development of the hybrid organic/inorganic halide perovskites (HOIHP) by answering fundamental scientific questions with ramifications on potential applications of these materials. We had planned a set of experiments with the objectives to: (i) study the charge transport in HOIHP films and single crystals in bulk and field-effect transistor (FETs) to advance the basic understanding of charge transport in these materials, (ii) Improve the FET performance by tuning the device design and processing, and (iii) Synthesize new Pb-free hybrid perovskites and incorporate them in opto-electronic applications.

What was accomplished towards achieving these goals?

Accomplishment 1: We lowered the trap densities in perovskite FETs and achieved high mobility and 'band-like' transport

Hybrid organic-inorganic halide perovskites were incorporated in a wide variety of devices ranging from solar cells to light emitting diodes, lasers, spintronic devices and more. By careful device design, we were able to fabricate the first working perovskite field-effect transistor (FET), with support from this grant.¹ This device operated both in the p-type and n-type regime, with typical charge carrier mobilities around $1 \text{ cm}^2/\text{Vs}$ at room temperature, in the dark, and reaching mobilities as high as $10 \text{ cm}^2/\text{Vs}$ for several samples. The variations in electrical properties result from charge trapping at the semiconductor/dielectric interface. Therefore, we further focused on an in-depth study of the trap states by following the dependence of the carrier mobility on the electric field, i.e. the Poole-Frenkel (PF) effect. We fabricated bottom-contact, top-gate FETs with 5 nm Ti/ 50 nm Au source and drain electrodes treated with various self-assembled monolayers (SAMs), Cytop gate dielectric and Al or Au top-gate electrode. Since one of the main sources for the traps arises from the microstructure of the hybrid perovskite film, we tuned the processing parameters (SAM treatment, method for perovskite deposition, solution concentration, type of solvent, etc) to vary the quality of this layer. The following SAMs were used: Pentafluorothiophenol (PFBT); 4-(trifluoromethyl)thiophenol (TFBT); and 2,3,5,6-tetrafluoro-4-(trifluoromethyl) benzenethiol (TTFP). For comparison we also fabricated FETs with no treatment.

We followed the evolution of carrier mobility, μ with the applied electric field, E using the PF relation: $\mu = \mu_0 \exp(\gamma\sqrt{E})$, from which we determined the PF pre-factor, γ . Here E is given by the applied V_{DS} , namely $E = V_{DS}/L$, where L is the channel length, and μ_0 is the zero field mobility. In Figure 1a we show the mobility evolution with the applied field for devices of varying sample quality: a strong field-dependence indicates transport dominated by ‘extrinsic defects’. Indeed, the devices that showed the highest mobility (black), also showed the weakest field dependence of mobility (γ_1). As the trap densities increased, the PF pre-factor increased as well, $\gamma_1 < \gamma_2 < \gamma_3$. In Figure 1b we plot the mobility dependence on γ obtained from over 50 FETs of different trap densities. An inverse correlation between mobility and γ can be clearly observed. The mobility increases over five orders of magnitude as a result of decreasing γ by about 20 times. This result provides conclusive evidence that trapping of charge carries is an important source of scattering. Inhibiting charge transport in hybrid perovskites, and minimizing it could give rise to high performance devices. In addition, we have also observed that very good operational and environmental stability is characteristic for the higher mobility devices.

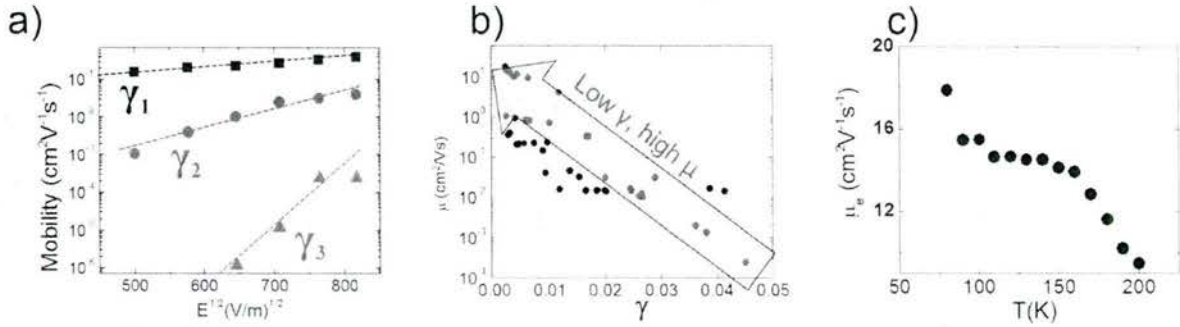


Figure 1: Field-effect mobility in perovskite field-effect transistors. a) Mobility versus lateral electric field for devices of low (black), medium (red) and high (blue) trap densities. The slope yields the Poole-Frenkel factor γ . b) Dependence of charge carrier mobility on the PF factor. c) Evolution of mobility with temperature showing band-like transport in perovskite transistors.

The charge carrier mobility dependence on temperature incorporates important information on the charge transport mechanism in the semiconductor: an increase in mobility with decreasing temperature that obeys a power-law relation, $\mu \sim T^{-n}$, with $0.5 \leq n \leq 3$ is typical to a ‘band-like’ transport. In this model, the interaction of the delocalized charge carriers with the lattice phonons represents the main scattering process. A thermally activated mobility, described by an Arrhenius-like relation, $\mu \sim \exp[-E_A/kT]$, where E_A stands for the activation energy, is generally a signature of disorder that has been described in terms of the ‘multiple trapping and release’ (MTR) model, or variable range hopping (VRH) model. Indeed, for the devices of highest room-temperature mobility and lowest defect density, we were able to measure an *increase in mobility* with lowering the temperature (see Figure 1c). This is the first time where ‘band-like’ transport was measured in

hybrid perovskite transistors; it results from an *aggressive* lowering of the trap densities at the semiconductor/dielectric interface. This was achieved by carefully controlling the perovskite film microstructure, coupled with the use of an inert organic dielectric, and the use of SAMs to control the film order and charge injection.

Accomplishment 2: Transport studies using time-of-flight measurement

For studying carrier mobility, μ of methyl-ammonium lead trihalide perovskites (MAPbX_3) using the time of flight (TOF) method, it is required to perform the measurements on a sample of thickness larger than can be generated through either solution-based or evaporation techniques. We succeeded in growing such single crystals of MAPbBr_3 , and more recently also MAPbI_3 , with dimensions of 1-4mm to obtain the large transport lengths, L necessary for TOF. Planar diode structures have been fabricated by evaporating a semi-transparent (30nm) Au layer on one surface of the crystal as anode. Ag-epoxy is used as cathode and also as heat sink the crystal to the 'cryostat sample holder' for temperature control during the measurements. This device architecture allows for measurement of electron transport, as photo-excitation is through the electron-injection-blocking Au contact. These contacts are not ideal, and later work involved improvement of the diode structure that allowed for studying hole transport by replacing the Ag-epoxy with ETL/Al(30nm), where ETL is a few nm thin electron-transport-layer such as C_{60} .

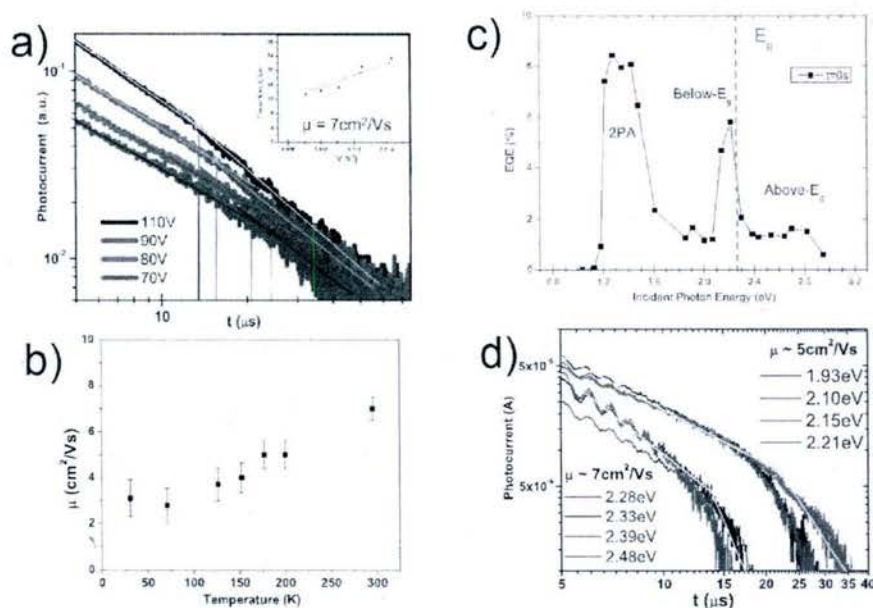


Figure 2. (a) Log-log plot of PC vs. time at different applied voltages for 1 mm thick MAPbBr_3 crystal. The lines indicate asymptotes of the two power laws, the intersections of which (squares) are indicated by the vertical lines. Inset: The extracted t_{tr} in μs vs. $1/V$. (b) Values of μ extracted at different temperatures. (c) Percent of incident photons converted to electrons (EQE) vs. the excitation photon energy. The red-dashed line indicates the lower bound of the optical band gap E_g . (d) PC transients for several different incident photon energies.

Figure 2a shows a typical photocurrent (PC) decay of Au(30nm)/MAPbBr₃(1mm)/Ag-epoxy device following photo-excitation with a ns-pulsed laser excitation at 450nm under reverse bias of 100V. The signal is dominated by an exponential decay at short times that is determined by the RC-time constant of the experimental apparatus ($\tau_{RC} = 1.6\mu s$). At times longer than τ_{RC} , the PC transient shows a long tail that is a sign of dispersive transport. The data is plotted on a log-log scale in the figure; the distinctive ‘kink’ that displays the change in power law is observed. The kink moves to shorter times as the voltage applied is increased (Fig. 2a, inset) and can be used to extract a mobility value if the intersection of the asymptotes of the two power laws is used as the carrier transit time, t_{tr} , in the standard equation for $\mu (= L^2/(V*t_{tr}))$; although in this case the mobility will be a function of time and sample thickness and the determined value represents that of the most mobile carriers. The mobility value extracted in this case at room temperature is $\mu = 7\text{cm}^2/\text{Vs}$. We found similar results in MAPbI₃ single crystals. This data is consistent with published reports. However, in those works the implications of ‘dispersive transport’ was not considered. Dispersive transport results from multiple-trapping and release events in the band-tails of the density of states (DOS) near the mobility-edge, which is experienced by carriers as they move through the sample. Considering the numerous claims of excellent transport properties and low-trap state densities reported for these materials, the origin of this dispersion is intriguing.

Further investigation into the origin of the dispersive nature of transport in single crystal MAPbX₃ crystals was obtained by varying the temperature of the device. The carrier mobility extracted from MAPbBr₃ crystals varies little with temperature, showing a slight *decrease* in μ with *decreasing* temperature Figure 2b. This is consistent with a trap-limited transport that is enhanced by activation from the phonon bath. The fact that the transients remain dispersive at room temperature suggests a relatively deep trap depth.

The excitation for photogeneration of current (i.e. photocurrent, PC) was provided by a wavelength-tunable ~5 ns pulsed laser system. This allowed us to characterize carrier transport as a function of their initial position within the DOS of the hybrid perovskite sample. We found an interesting dependence of the PC on the incident photon energy, which is displayed in Figure 2c. The dashed line indicates the transmittance edge of the crystal representing the optical band gap, E_g . It can be clearly seen that much larger PC is generated with below-gap excitation than above gap excitation, and that PC can, in fact, also be generated by *two-photon absorption* (2PA) near $(1/2)E_g$. The smaller PC for above- E_g excitation is consistent with reports on photo-detectors made from such crystals, attributed to surface recombination facilitated by surface traps. The more efficient PC generation (per incident photon) through 2PA is due to bulk volume generation in the crystal, in combination with dispersive transport that leads to a higher effective mobility for carries generated closer to the collecting electrode. Figure 2d shows the characteristic PC transients, for above-gap and below-gap excitation. It is evident from the figure that the carrier transport is faster when excited above-gap. This is consistent with the excess energy assisting in the release from trap states.

Accomplishment 3: Perovskite FET transistors on hydrophobic surfaces

Solution-processable electronic devices are highly desirable due to their low cost and compatibility with flexible substrates. However, they are often challenging to fabricate due to the hydrophobic nature of the surfaces of the constituent layers. To date, most of solution-deposited devices had only one or a few layers deposited from solution, using simple methods such as inkjet printing, spin casting, or spray coating, while the other layers were obtained by electron-beam evaporation, thermal evaporation, or other complex technologies, which significantly increased the overall cost of fabrication and limited their applicability. This compromise was necessary, however, because the hydrophobic nature of many solution-deposited compounds precluded the deposition of consecutive layers onto their surface. In this project, we developed a method for tailoring the surface properties of the highly hydrophobic dielectric Cytop by applying a treatment with a protein solution to improve its wettability and allow for subsequent solution processing at its surface. We find that this treatment does not alter the electrical properties of the Cytop layer, but increases its surface energy sufficiently to allow for solution-deposition of other layers on its surface. We then fabricate bottom-gate FET devices on the protein/Cytop dielectric with halide perovskite semiconductors.

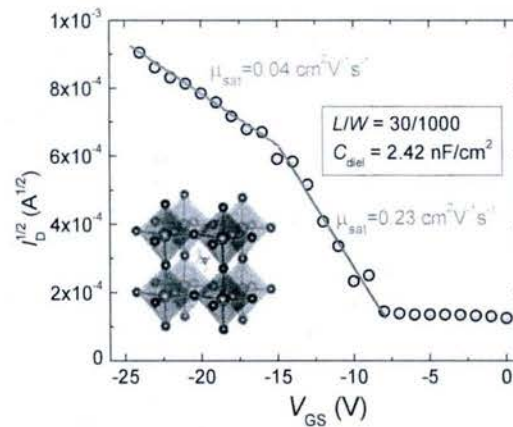


Figure 3. Drain current versus the applied gate-source voltage in the saturation regime, at room-temperature, for a FET with protein/Cytop bottom gate. The device geometry and dielectric capacitance, as well as the perovskite structure are include in the inset.

A typical transfer curve is shown in Figure 3. The inset in this figure represents the crystal structure of the perovskite, with the Pb^{2+} cations and the halide anions sitting at the centers and corners of the octahedra, respectively; and the methylammonium organic cations in the interstices. The current-voltage characteristics shown here deviates from a straight line necessary in order to use equation (1) for mobility estimation. This type of behavior results from severe contact effects, which we have discussed in detail elsewhere.⁴¹ In the low-voltage regime we obtained $\mu = 0.23 \text{ cm}^2\text{V}^{-1}\text{s}^{-1}$, a value which is most likely an overestimation of the real mobility of this device, while the value obtained at high voltages, $\mu = 0.04 \text{ cm}^2\text{V}^{-1}\text{s}^{-1}$ is a more conservative estimation. Both

values, however, are lower than the mobility obtained on the same perovskite layer, but with Cytop top dielectric, $\mu = 1.3 \text{ cm}^2\text{V}^{-1}\text{s}^{-1}$. This is probably due to increased density of trapping states at the semiconductor/dielectric interface because of the insertion of the protein layer. In addition, while for the top-gate devices with neat Cytop dielectric layer we observed ambipolar transport, we found that the electron transport was inhibited at the hydrophilic interface created by the protein treatment.

Accomplishment 4: Large-area electronics on hybrid perovskites

Impressive demonstrations in the field of hybrid perovskite electronics have generated excitement in studying these type of materials. But, with a few exceptions, the properties of devices reported in the literature can only be reproduced over small areas. Achieving good performance and uniformity over large-areas is hard due to the lack of processing methods that maintains film quality over large areas. Scaling up from laboratory-based devices to large-area electronics without compromising performance is one of the big challenges faced by the field. *Because of this, we focused our efforts not only towards improving device performance, but also in ensuring that this performance is recovered over large areas, without exorbitant fabrication costs.* We employed ‘spray-coating’ for the deposition of the hybrid perovskite layer. This is a fast, high-throughput manufacturing method that is easily scalable to large areas.

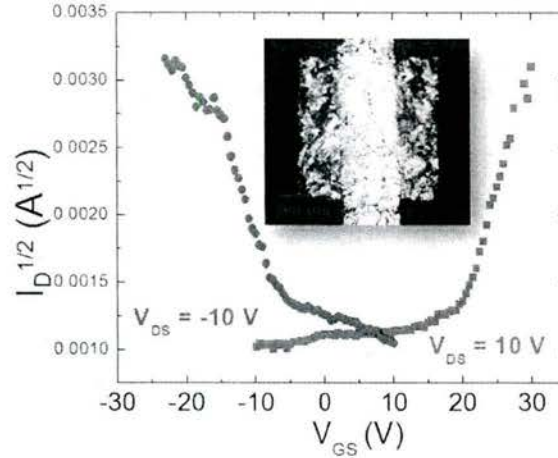


Figure 4. Evolution of the drain current versus the drain voltage in spray-deposited perovskite field-effect transistors in the saturation regime for p-type (red) and n-type (blue) operation. The inset shows a photo of the device.

To perform ‘spray-coating’, we started with the Si/SiO₂/Ti/Au substrates, similar to our spin-coating studies. The semiconductor was dissolved in a solvent and the solution was directed toward the substrate with an air brush held at a controlled distance h above the substrate. The solution was

atomized by applying pressure to high-purity Ar, the transporting gas. We learned that film formation by 'spray-coating' method is critically affected by such processing details as solution concentration, type of solvent (boiling point, vapor pressure, viscosity), spraying distance, transporting gas pressure, substrate temperature, and substrate surface energy. Consequently, we systematically modified these parameters to improve film morphology. Surface energy was also modified using SAMs. We found that at reduced rates, obtained using a small nozzle opening and/or reduced Ar pressure, femtoliter-sized droplets landed on the surface forming domains that dried independently without particularly good interconnectivity. At very large deposition rates, a continuous wet layer formed. Therefore, by trial and error we determined the intermediate rates, which allowed us to obtain high quality films.

Figure 4 shows the evolution of the source-drain current with the applied voltage for a perovskite FET in the saturation regime. The measurements were obtained in the dark, in air and at room-temperature. The red curve corresponds to the p-type operation, and the blue one to the n-type operation. The mobility calculated from these measurements is $\mu = 4 \text{ cm}^2/\text{Vs}$ for both electrons and holes. The inset shows a photo of the device. Whereas in this work only the semiconductor layer was deposited by 'spray-coating', and conventional deposition methods were used for the other layers, this work demonstrates the viability of the approach. In future studies, we will leverage our results obtained on all-sprayed organic thin-film transistors to achieve high-performance *all-sprayed* perovskite FETs.

Accomplishment 5: Synthesis of novel hybrid organic-inorganic perovskites

Quasi-two dimensional (2D) materials often show superb photophysical properties, such as large exciton binding energy, enhanced absorption with respect to the bulk, low threshold stimulated emission, and notable optical nonlinearities. These observed properties are also strongly dependent on the number of layers present in the 2D system. Until recently, quasi-2D organo-lead perovskites were reported as potential materials that can overcome the overall low stability observed in their 3D counterparts. However, little is known about the structural, optical, electronic properties of these 2D organo-lead perovskites keeping in mind that their physical properties are far more tunable and flexible when compared to 3D organo-lead perovskites. During this grant support period we have studied the 3D to 2D structural transition of organo-lead perovskites by systematic modifying the organic moiety that is present in these systems. This 3D to 2D structural transition is triggered by the substitution of the small methylammonium organic cation by bulkier organic ammonium cations (e.g., ethylammonium (EA^+), propylammonium (PA^+), and butylammonium (BA^+), phenylethylammonium (PhEA^+)), which put considerable steric strain on the overall lattice of the perovskite structure (see Figure 5). This sub-nanometer layered system promotes the generation of stable excitons through electronic confinement, making these materials unique in their charge dynamics and transport, see Figure 5.

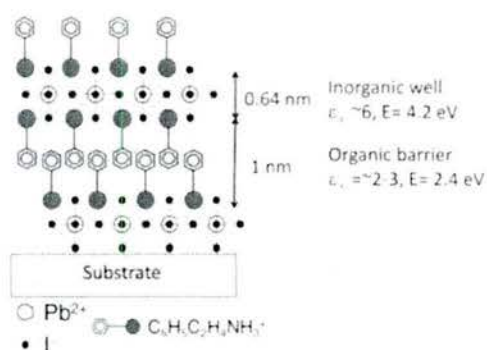


Figure 5: Schematic of the 2D organic-inorganic perovskite PEPI that shows naturally formed multiple quantum wells comprised of alternating layers of inorganic PbI_4 and organic barriers

Figure 6 depicts X-ray diffraction (XRD) spectra of several perovskites thin films with different organic cations that were synthesized at the University of Utah (UofU). These films were prepared by spin-coating a solution comprised of 1:1 molar ratio of cation: PbI_2 for NH_4PbI_3 , MAPbI_3 , and EAPbI_3 and 2:1 molar ratio of cation: PbI_2 for perovskites $(\text{PA})_2\text{PbI}_4$, and $(\text{BA})_2\text{PbI}_4$, in dimethylformamide (DMF). The XRD spectra in Figure 6 show the formation of low-dimensional layered structures when the methylammonium cation is replaced with larger cations. These low dimensional structures were formed by slicing along the (110) face of the 3D perovskite in such a way that the c-axis (00 l) is the dominant phase of the 2D perovskite layers. Moreover, introduction of a larger cation such as ethylammonium (EA^+) within the PbI_6 inorganic cage shows the formation of a highly oriented system aligned along the (002) crystallographic plane (Figure 6, brown line). The alignment along this plane suggests the formation of a layered perovskite system. Furthermore, as shown in Figure 6, the major c-axis (002) crystallographic plane shifts to lower 2θ values thus, suggesting a larger d-spacing as the perovskites transition to a layered structure. We believe the observed lattice expansion is due to the introduction of stronger van der Waals interactions within the larger cations and the inorganic cage.

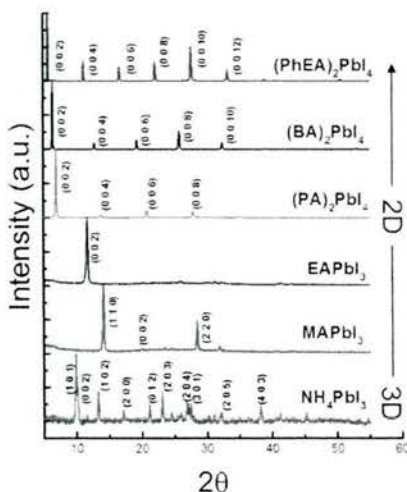


Figure 6. XRD patterns of various perovskites structures that are based on different organic cations. All diffraction peaks are indexed according to previous literature values.

The optical properties observed when transitioning from 3D to 2D perovskites are dominated by the creation of tightly bound excitons in the 2D perovskites. 2D perovskites have densely packed layers of opposing dielectric constants acting as quantum wells for excitons, localizing the charges in the layers (Figure 5). Because of this localization, the exciton binding energy (E_b) generally increases as quantum confinement increases, resulting in distinct optical spectral features that help identifying the 2D band structure. For perovskites with excitons as the dominant photoexcitation species, the absorption is concentrated below the gap in a narrow spectral feature since it steals the oscillator strength from the interband absorption (see Figure 7).

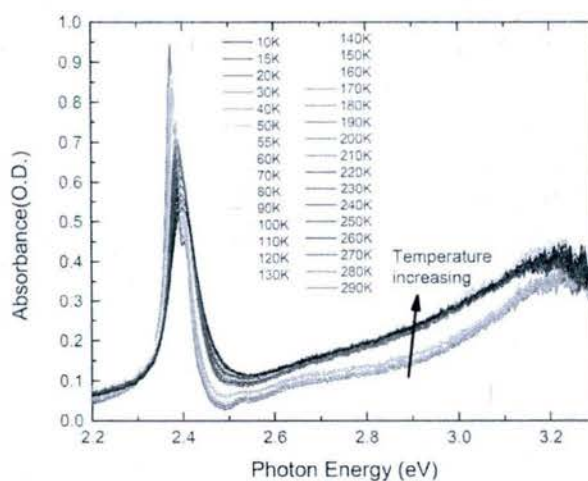


Figure. 7: The absorption spectrum of PEPI film measured at temperatures ranging from 10 K to 290 K, as denoted. The dominant 1s exciton absorption band at ~ 2.38 eV steals its oscillator strength from the interband absorption edge at ~ 2.58 eV. The 2s exciton band at 2.53 is also clearly seen. The 1s exciton binding energy in PEPI is thus estimated as ~ 200 meV, whereas it is ~ 50 meV for the 2s excitons, in agreement with Bohr's 'hydrogen model'.

What opportunities for training and professional development did the project provide?

Three graduate students from Wake Forest University and one graduate student from University of Utah, that have been partially supported by this grant were involved in this project. The graduate students working on this project are pursuing a PhD in Physics. WFU graduate student Yaochuan Mei designed, fabricated and tested FET devices at room-temperature and low-temperatures. He performed the Poole-Frenkel studies. He also fabricated and characterized thin-film transistors using spray-deposition and he characterized their electrical properties. Ge graduated in the summer of 2016. His project was continued by a second year graduate student, Andrew Zeidell, who focused on the fabrication of perovskite FETs on hydrophobic surfaces treated with protein solutions. UofU graduate student Qingji Zeng helped perform the TOF measurements.

Postdoctoral researcher Dr. Charlie Zhang at UofU fabricated the conventional and Pb-free perovskites and evaluated their structural properties; he also synthesized the 2D perovskite PEPI.

Postdoctoral researcher Dr. Evan Lafalce at UofU performed the TOF studies. Profs. Vardeny and Jurchescu supervised the students and postdocs and directed the project.

How were the results disseminated to communities of interest?

The results have been disseminated using multiple venues, which included presentations, preparation of journal articles, one dissertation, as well as outreach activities. The PIs have given several invited talks at conferences on the project topic, including at the APS March meeting and MRS (2016, Jurchescu), and at ICSM 2016, Guangzhou, China in June 2016 (Vardeny). The students and postdocs gave talks and presented posters at conferences.

Vardeny organized a focused session on Hybrid Perovskites at the 2016 March APS meeting in Baltimore, while Jurchescu organized this session at the 2017 March APS meeting in New Orleans. Each symposium had three full sessions that were very well attended (~150 participants). Jurchescu is an associate editor for the Journal of Electronic Materials and a member of the editorial board of Scientific Reports (Nature publishing group).

Technology Transfer

Hybrid halide perovskite-based Field-effect transistors, Yaochuan Mei, Charlie Zhang, Valy Vardeny, Oana Jurchescu, application number 62252871, provisional patent, 11/09/2015.

Participants

Oana Diana Jurchescu

Faculty

1 month

National Academy Member? N

Zeev Valentine Vardeny

Faculty

1 month

National Academy Member? N

Students

Two graduate students from Wake Forest University (Yaochuan Mei, and Andrew Zeidell).

One graduate student earned his PhD degree in 2016 (Yaochuan Mei).

One physics graduate student from the University of Utah (Qingji Zeng).

Publications

Y. Mei, C. Zhang, Z.V. Vardeny and O.D. Jurchescu, *Electrostatic gating of hybrid halide perovskite field-effect transistors: balanced ambipolar transport at room-temperature*, **MRS Commun** 5, 297 (2015).

J. W. Ward, H. L. Smith, A. Zeidell, P. J. Diemer, S. R. Baker, H. Lee, M. M. Payne, J. E. Anthony, M. Guthold, and O.D. Jurchescu, *Solution-Processed Organic and Halide Perovskite Transistors on Hydrophobic Surfaces*, **ACS Applied Materials & Interfaces**, in revisions

E. Lafalce, C. Zhang, X. Liu, and Z. V. Vardeny, *On the role of intrinsic ions accumulation in the photocurrent and photo-capacitive responses of MAPbBr₃ photodetectors*, **ACS Applied Materials and Interfaces**, December 2016; [10.1021/acsami.6b11925](https://doi.org/10.1021/acsami.6b11925).